Incomplete Label Multi-task Deep Learning for Spatio-temporal Event Subtype Forecasting

Yuyang Gao
George Mason University
ygao13@gmu.edu

Liang Zhao
George Mason University
lzhao9@gmu.edu

Lingfei Wu
IBM Research
wuli@us.ibm.com

Yanfang Ye
West Virginia University
yanfang.ye@mail.wvu.edu

Hui Xiong
Rutgers University
hxiong@rutgers.edu

Chaowei Yang
George Mason University
cyang3@gmu.edu

Abstract

Due to the potentially significant benefits for society, forecasting spatio-temporal societal events is currently attracting considerable attention from researchers. Beyond merely predicting the occurrence of future events, practitioners are now looking for information about specific subtypes of future events in order to allocate appropriate amounts and types of resources to manage such events and any associated social risks. However, forecasting event subtypes is far more complex than merely extending binary prediction to cover multiple classes, as 1) different locations require different models to handle their characteristic event subtype patterns due to spatial heterogeneity; 2) historically, many locations have only experienced a incomplete set of event subtypes, thus limiting the local model's ability to predict previously "unseen" subtypes; and 3) the subtle discrepancy among different event subtypes requires more discriminative and profound representations of societal events. In order to address all these challenges concurrently, we propose a Spatial Incomplete Multi-task Deep leArning (SIMDA) framework that is capable of effectively forecasting the subtypes of future events. The new framework formulates spatial locations into tasks to handle spatial heterogeneity in event subtypes, and learns a joint deep representation of subtypes across tasks. Furthermore, based on the "first law of geography", spatially-closed tasks share similar event subtype patterns such that adjacent tasks can share knowledge with each other effectively. Optimizing the proposed model amounts to a new non-convex and strongly-coupled problem, we propose a new algorithm based on Alternating Direction Method of Multipliers (ADMM) that can decompose the complex problem into subproblems that can be solved efficiently. Extensive experiments on six real-world datasets demonstrate the effectiveness and efficiency of the proposed model.

Introduction

Spatio-temporal societal events such as disease outbreaks and organized crime have a significant impact on society. The ability to successfully forecast future spatial events of this nature would thus be extremely beneficial for decision makers seeking to avoid, control, or alleviate the associated social upheaval and risks. Spatial social event forecasting is a fast-growing research area that typically forecasts the *occurrence* of future spatial events, namely whether or not a particular spatial event will happen. However, in many applications simply forecasting the *occurrence* of an event is not enough. Knowledge regarding the *subtype* or *category* of a future event is vital if decision makers are to achieve accurate and optimal resource allocation. For example, Figure 1 shows the percentage of six pollutant subtypes that feature in air pollution events based on the most frequently detected primary pollutants in Shenzhen, China in Summer 2013 (Xia et al. 2016). Local Environmental Monitoring Centers try to identify which pollutant source causing the most harm to public health and take appropriate action. For instance, when the pollutant subtype is $PM2.5$ (atmospheric particulate matter with a diameter less than 2.5 micrometers), the government can suggest that people who are sensitive to small particles wear gauze masks to protect themselves. On the other hand, when the subtype is O_3 (trioxygen), government agencies need to alert people to avoid going outside when the O_3 concentration is highest. Thus, successful forecasting of the pollutant subtypes provides more specific information that enables practitioners to allocate resources that will address public health issues with the specific primary pollutant source most effectively.

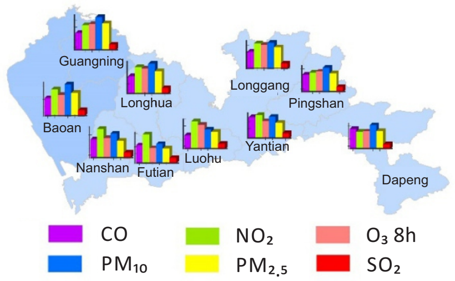

Figure 1: Relative amounts of six air pollutant subtypes in 10 districts in Shenzhen, China, 2013 (Xia et al. 2016).

Most of the existing work in this area such as (Ramakrishnan et al. 2014; Zhao et al. 2015a) has focused primarily on the event occurrence rather than engaging in the study of the various event subtypes, more detailed literature survey is provided in the supplementary material[1]. A few primitive studies (Chen et al. 2013; Ning et al. 2016) have started to explore this open problem, typically by applying simple multi-class classification techniques. However, spatial event subtype forecasting is far more complex than simply extending the binary classification problem into a multi-class set-

[1] http://mason.gmu.edu/~lzhao9/materials/papers/supp_AAAI2019.pdf

ting, because of several crucial challenges are involved: **1) Spatial heterogeneity and correlation of event-subtype patterns**: Different locations have different characteristics, such as population, climate and administrative policies. In addition, spatial locations are correlated in terms of their spatial topology. According to the well-known "first law of geography" (Cressie 2015), the event subtype pattern should be more similar in nearby locations than in those further-away. **2) Incomplete labels in spatial event subtypes**: Due to the large number of potential subtypes and the limited availability of historical data, there may be new subtypes that do not appear in a specific location in the training set. This means the predictive model for a specific location will be unable to forecast these unseen subtypes in the future, which could lead to significant problems especially for rare but destructive events, such as pandemics and terrorist attacks. **3) Difficulties in representing event subtype patterns**: The conceptual and semantic discrepancy between event subtypes could typically be too subtle to discriminate based solely on manually-defined features such as bag-of-words representations. This representation is both sparse and high-dimensional and hence suffers from *curse of dimensionality* (Bellman 2013) and low efficiency.

In this paper, we propose a novel Spatial Incomplete Multi-task Deep leArning (SIMDA) framework for spatial event subtype forecasting that addresses all the above challenges. The main contributions of our study are as follows:

1. **Developing a new deep-based framework for societal event subtype forecasting.** We formulate event subtype forecasting for multiple locations as a spatial incomplete multi-task learning problem and propose a novel deep-based framework that learns profound representations of event subtypes across tasks. We enforce shared latent feature representations for different locations while preserving heterogeneity in their event subtype patterns.
2. **Proposing a model that enforces spatial event subtype patterns.** Based on the first law of geography, we enforce similar event subtype patterns among spatially-closer tasks via a novel deep regularization term that is proved to be theoretically equivalent to the ratio of the probabilities of the event subtypes distribution patterns in nearby locations. In addition, the newly proposed deep regularization term enjoys better scalability with high-dimensional data and is thus more capable of handling complex real world problems effectively and efficiently.
3. **Developing an efficient algorithm for solving new non-convex and strongly-coupled problems.** To solve the proposed model's objective function, which is non-convex and highly-coupled, we propose a new algorithm based on the Alternating Direction Method of Multipliers (ADMM) that decomposes the original complex problems into subproblems that can be solved efficiently with analytical solutions and conventional stochastic optimization.
4. **Conducting comprehensive experiments to validate the effectiveness and efficiency of the proposed model.** Extensive experiments on six real-world datasets in two domains, civil unrest and air pollution event forecasting, demonstrate that the proposed models outperform other comparison methods in different application domains. In addition, sensitivity and qualitative analyses are provided to demonstrate the effectiveness of the proposed regularization term.

Problem Setup and Preliminary Setups

Problem Setup

Suppose there are $\mathcal{S}$ spatial locations (e.g., cities, states) in a country of interest and T denotes all the time intervals. The spatio-temporal social indicator data (e.g., social media, news, pollutant factors) for location s and time interval t (e.g., one day) can be formulated as $X_{s,t} \in \mathbb{R}^{1\times D}$, which denotes a D-dimension feature vector whose i-th element is a feature value (e.g., the term frequency or index value).

The event subtype at location s and time t is defined as an nominal response $Y_{s,t} \in \{\mathcal{C}_1, \mathcal{C}_2, ..., \mathcal{C}_K\}$, where $\mathcal{C}_1, \mathcal{C}_2, ..., \mathcal{C}_K$ are class labels and K is the total number of event subtypes. Notice that here a "non-event" will also be defined as a default subtype when no event happens.

Given the input data $X_{s,t}$ for a specific location s and a time interval t, the goal is to predict the subtype of a future event, denoted by $Y_{s,\tau}$, for the same location s and a future time interval τ, where $\tau = t + p$ and $p > 0$ is the lead time. In this paper, the default time intervals t is per day and the lead time p is one day ahead unless otherwise specified. Formally, this problem is equivalent to learning a mapping from input data to a future event subtype $X_{s,t} \rightarrow Y_{s,\tau}$.

Preliminaries

To address this issue, multi-class classification models (Wu et al. 2018) such as multinomial logistic regression (also known as softmax regression) and neural networks (Xu et al. 2018) are commonly used to solve the problem due to the nature of predicting multiple outputs with a single model.

The objective function of our problem with the softmax regression formulation is as follows:

$$\mathcal{L}(\theta) = -\frac{1}{\mathcal{S}T}\left(\sum_{s}^{\mathcal{S}}\sum_{t}^{T}\sum_{k=1}^{K}\mathbf{1}\{Y_{s,t}=k\}\log\frac{e^{X_{s,t}\theta_k^T}}{\sum_{c=1}^{K}e^{X_{s,t}\theta_c^T}}\right) \quad (1)$$

where $\theta \in \mathbb{R}^{K\times D}$ is the parameter set of the model , $\theta_k \in \mathbb{R}^{1\times D}$ denotes the weight coefficients for class k, and $\mathbf{1}\{\cdot\}$ is the indicator function. For example, suppose the event subtype for location s at time t is k, then $\mathbf{1}\{Y_{s,t} = k\} = 1$ while $\mathbf{1}\{Y_{s,t} = j\} = 0$ for any $j \neq k$.

The model proposed in Equation (1) suffers from a critical challenge: all the locations share a single *weight coefficient* vector θ, hence the model cannot handle any spatial heterogeneity in the event subtype for different locations.

To address this challenge, we can extend Equation (1) to create a location-specific model, where each location s has its own weight coefficient set, denoted as $\Theta_s \in \mathbb{R}^{K\times D}$. Here, $\Theta_{s,k} \in \mathbb{R}^{D\times 1}$ denotes the weight coefficients for location s and for class k and the objective function of the location based softmax regression formulation is as follows:

$$\mathcal{L}(\Theta) = -\frac{1}{\mathcal{S}T}\left(\sum_{s}^{\mathcal{S}}\sum_{t}^{T}\sum_{k=1}^{K}\mathbf{1}\{Y_{s,t}=k\}\log\frac{e^{X_{s,t}\Theta_{s,k}^T}}{\sum_{c=1}^{K}e^{X_{s,t}\Theta_{s,c}^T}}\right) \quad (2)$$

However, the above formulation is still insufficient as Equation (2) assumes all the locations are independent, even

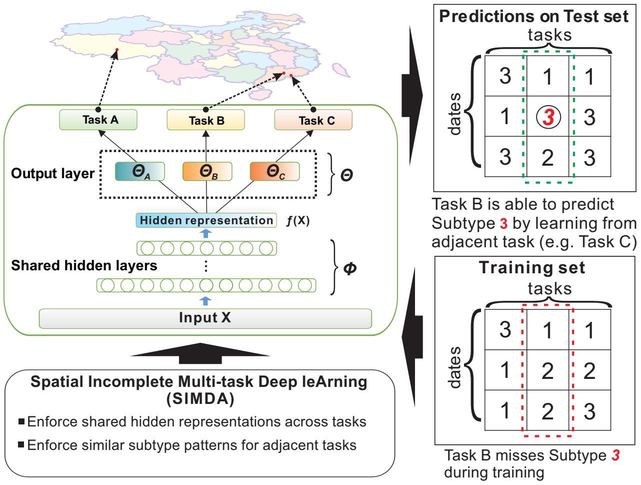
Predictions on Test set
tasks
dates
3 1 1
1 3 3
3 2 3
Task B is able to predict Subtype 3 by learning from adjacent task (e.g. Task C)
Training set
tasks
dates
3 1 1
1 2 2
1 2 3
Task B misses Subtype 3 during training
Task A
Task B
Task C
Output layer
Θ_A
Θ_B
Θ_C
Θ
Hidden representation
f(X)
Shared hidden layers
Φ
Input X
Spatial Incomplete Multi-task Deep leArning (SIMDA)
Enforce shared hidden representations across tasks
Enforce similar subtype patterns for adjacent tasks

Figure 2: Flowchart of the proposed SIMDA framework

though some spatial correlations will exist among the various locations in terms of the event subtype pattern, as shown in Figure 1. Also, Equation (2) tries to learn an individual parameter set Θ_s for each location s, which can dramatically reduce the training sample size for a given location model. Furthermore, due to the large number of potential subtypes and the limited amount of local historical data, there may be unseen subtypes that have not appeared in a specific location within a time period. For example in Brazil, there were no education or medical related protests in city Belo Horizonte during the time period from July, 2013 to February, 2014. This means the specific model for the city Belo Horizonte will not be able to forecast these two subtypes in the future.

SIMDA Model

Incomplete Multi-class Spatial Regularization

In order to jointly handle the spatial heterogeneity issue in Equation (1) and spatial correlation issue in Equation (2), multi-task learning technique is leveraged which can jointly learn the shared characteristics among tasks while preserve the exclusive patterns for each task (Yuan, Zhou, and Yang 2018; Thrun and OSullivan 1998). (Zhao et al. 2015b) have demonstrated the utility of applying a Multi-Task Learning framework for forecasting spatiotemporal event occurrence. (More detailed literature survey is included in the supplemental material.) However, when forecasting event subtype, where multi-class classification problem is combined with multi-task learning, each task has only a limited number of samples and thus in practice not every task has a complete set of labels in the training set. For example, in Figure 2 the bottom right box contains an example of a set of training data labels (event subtypes). Only task C has a complete set of labels, the other two tasks are both missing one class. Consequently, the weight coefficient associated with the missing event subtype k cannot be learned during training and the model is not capable of predicting the missing event subtypes. Note that this issue becomes more severe as the number of class labels increases.

In order to address this problem, we propose allowing correlated tasks to adaptively complement each other's missing classes. This means that we first need to determine the correlation among tasks. Based on the first law of geography, namely "everything is related to everything else, but near things are more related than distant things"(Cressie 2015), nearby locations will tend to be more similar to each other.

For a time interval t, given two locations i and j that are close in geo-spatial distance, the probability of the event subtype $\mathcal{C}_a$ at location i denoted as $P(Y_{i,t} = \mathcal{C}_a|X_{i,t})$, will be similar to that at location j, leads to the following equation:

$$P(Y_{i,t} = \mathcal{C}_a|X_{i,t}) \approx P(Y_{j,t} = \mathcal{C}_a|X_{j,t}) \qquad (3)$$

Likewise, the ratio of the probability of the event subtype at location i being equal to event subtype $\mathcal{C}_a$ compared to event subtype $\mathcal{C}_b$, should also be similar to that at location j. This can be expressed as:

$$\frac{P(Y_{i,t} = \mathcal{C}_a|X_{i,t})}{P(Y_{i,t} = \mathcal{C}_b|X_{i,t})} \approx \frac{P(Y_{j,t} = \mathcal{C}_a|X_{j,t})}{P(Y_{j,t} = \mathcal{C}_b|X_{j,t})} \qquad (4)$$

The posterior probability $P(Y_{i,t} = \mathcal{C}_a|X_{i,t})$ can be equivalently represented by any multi-class based models. The similarity pattern based on the ratio of the probability above can thus be equivalently denoted by input X and weight coefficient Θ based on Equation (2), as shown in Lemma 1.

Lemma 1. *Based on the model shown in Equation* (2) *, Equation* (4) *is theoretically equivalent to the following:*

$$X_i(\Theta_{i,a} - \Theta_{i,b})^T \approx X_j(\Theta_{j,a} - \Theta_{j,b})^T \qquad (5)$$

where i and j are two tasks that are close in geo-spatial distance and a and b are any two different event subtypes.

Proof. Please see our supplemental material for details. □

Therefore, we propose a new model to regularize the parameter based on Equation (4), and equivalently on Equation (5) by introducing a new regularization term for Θ based on spatial adjacency of the tasks. Mathematically, we propose the following model objective as follows:

$$\mathcal{L}(\Theta) + \frac{\beta}{2}\sum\nolimits_{s}^{S}\sum\nolimits_{i,j}^{C_k^2}\|X_s(\Theta_{s,i} - \Theta_{s,j})^T - \frac{1}{N_s}\sum\nolimits_{c}^{S} adj(s,c)X_c(\Theta_{c,i} - \Theta_{c,j})^T\|_2^2 \qquad (6)$$

where $\mathcal{L}(\Theta)$ is defined in Equation (2); the function $adj(s,c)$ defines the adjacency relation between s and c, which can be defined based on either spatial correlations such as spatial contiguity or spatial distance. N_s is the normalization term for location s such that $N_s = \sum_c^{S} adj(s,c)$. Here, the adjacent function is defined based on the physical distance and the well-known generalized RBF kernel (Haasdonk and Bahlmann 2004), as: $adj(s,c) = e^{-\gamma d(s,c)^2}$. The function $d(s,c)$ can be the physical distance between two spatial locations and γ is the scaling factor.

The proposed regularization term encourages adjacent tasks to have a similar ratio of the probability between any pair of event subtypes by ensuring the difference between the corresponding weight coefficients and input $X_i(\Theta_{i,\mathcal{C}_a} - \Theta_{i,\mathcal{C}_b})^T$ is similar for adjacent tasks. The regularization hyper-parameter β controls the importance of this term, which can be tuned via cross-validation.

Generalization to Deep Spatial Regularization

Softmax regression model can be seen as a special case of a neural network with 0 hidden layers. In this section, we propose a generalized Spatial Incomplete Multi-task Deep leArning (SIMDA) framework based on the deep architecture with arbitrary number of hidden layers. Figure 2 shows a flowchart of the proposed SIMDA framework. The framework adopts the idea of a shared bottom architecture that can learn the shared hidden representations of event subtypes across tasks. In addition, a spatial adjacency based deep regularization term is proposed to regularize the hidden representation learned by the shared hidden layers to enforce similar event subtype patterns for spatially adjacent tasks. For example, in Figure 2 Task B and Task C are closer than Task A, thus Task B and C can share knowledge of their subtype patterns and influence each other more strongly while Task A, which is further away, will not influence them as much. Consequently, with the help of this knowledge sharing, Task B is able to learn unseen event subtypes through Task C, mitigating the problem of incomplete subtype availability due to gaps in the local task training data.

More specifically, the generalized framework enjoys several advantages, including: **1) Greater discriminative and predictive power.** Based on the Universal Approximation Theorem (Hornik 1991), a simple neural network including only a single hidden layer can approximate any continuous function. More specifically, for event subtype forecasting, developing a better understanding of the subtle differences among event subtypes requires deep representations. **2) Better generalizability with deep spatial regularization.** Spatial regularization on the highly-concise feature representations learned by deep architecture can help boost the model generalizability considerably and it is especially important for deep learning applications that involve large dataset. **3) Better efficiency with respect to input dimensions.** Deep models learn highly-condensed and discriminative representations that typically have less dimensionality than row inputs, which means that generalized SIMDA frameworks can be more efficient to optimize.

In generalized SIMDA framework, suppose the function $f(\cdot)$ denotes the computation of the shared hidden layers and Φ denotes the parameter set of the network, the activation $f(X)$ is thus the hidden representations learned by the shared hidden layers. $f(X)$ is then passed as input to the task specific output layers with weight coefficient Θ to compute the final result, as shown in Figure 2. The similarity pattern based on the ratio of the probability in Equation (4) can thus be equivalently denoted by $f(X)$ and Θ, as shown in Theorem 1.

Theorem 1. *In the SIMDA framework, for any deep learning architectures that use the softmax function as their output layer, equation* (4) *is theoretically equivalent to the following:*

$$f(X_i)(\Theta_{i,a}-\Theta_{i,b})^T \approx f(X_j)(\Theta_{j,a}-\Theta_{j,b})^T \tag{7}$$

where $\Theta_{i,b}$ denotes the task specific output layer weight coefficient vector for task i and class $\mathcal{C}_b$.

Proof. Please see our supplemental material for details. □

Notice that Theorem 1 can be seen as a generalized form of Lemma 1 since Lemma 1 is a special case when function $f(\cdot)$ is the identity function $f(X)=X$. Moreover, since the regularization directly works on the output layer parameters set Θ and activation $f(X)$, there is no further restrictions of the network structures regarding the shared hidden layers. This means that the framework can be used with various deep learning architectures on the shared bottom layers (such as convolutional layers) and arbitrary activation functions (such as ReLU).

Mathematically, the Spatial Incomplete Multi-task Deep leArning (SIMDA) framework is as follows:

$$\mathcal{L}_D(\Phi,\Theta)+\frac{\beta}{2}\sum\nolimits_s^{\mathcal{S}}\sum\nolimits_{i,j}^{C_k^2}\|f(X_s)(\Theta_{s,i}-\Theta_{s,j})^T \tag{8}$$

$$-\frac{1}{N_s}\sum\nolimits_c^{\mathcal{S}} adj(s,c)f(X_c)(\Theta_{c,i}-\Theta_{c,j})^T\|_2^2$$

where we define $\mathcal{L}_D(\Phi,\Theta)$ as the general multi-task deep learning objective function; Φ is the weight coefficient parameter set for the shared hidden layers; Θ is the task specific output layer weights with $\Theta_{s,i}$ denoting the weights for task s and for predicting class $\mathcal{C}_i$.

Theorem 1 and the above model objective indicate that instead of directly applying the regularization based on input data X, SIMDA will learn the mapping from the input data from different tasks in a deep shared feature space and then apply the spatial regularization to the latent representation.

Algorithm

The problem in Equation (8) is nonconvex and parameters are tightly coupled together within the new regularization term. Moreover, the function $f(X)$ involves the shared neural network layers, with highly complex objective functions coupled with parameter set Φ. Instead of directly solving the whole problem with regularization, existing works typically first decompose it into subproblems which are much simpler or even with analytical solutions and hence ensures the efficiency. For example, several ADMM (Boyd et al. 2011) based methods has been proposed: (Kiaee, Gagné, and Abbasi 2016) applied ADMM on deep convolutional neural networks with sparse regularization and observed improvement on the optimization efficiency and overall performance; (Sun et al. 2016) proposed ADMM-NET for solving the general Compressive Sensing MRI problem. However, those algorithms are normally problem dependent and thus can not be directly used here. A new method is needed to solve our new problem which is highly challenging.

Thus, we propose a new algorithm based on ADMM that first decomposes the original problem into several simpler subproblems that can then be solved iteratively. Our algorithm ensures global optimal solutions with analytical solutions for all subproblems except the subproblem that includes the original deep model loss, which will be solved with Stochastic Gradient Descent (SGD) to get local optima. More details of the algorithm are presented as follows.

Based on the ADMM formulation, the original objective function of SIMDA can now be re-written as follows:

$$\mathcal{L}_D(\Phi,\Theta)+\frac{\beta}{2}\sum\nolimits_s^{\mathcal{S}}\sum\nolimits_{i,j}^{C_k^2}\|Z_s(V_{s,i}-V_{s,j})^T$$

$$-\frac{1}{N_s}\sum\nolimits_c^{\mathcal{S}} adj(s,c)Z_c(W_{c,i}-W_{c,j})^T\|_2^2 \tag{9}$$

$$\text{s.t. } \Theta=V, \Theta=W, Z=f(X)$$

Thus, by decoupling the output layer parameter set Θ that appears both in deep model loss and regularization term, the original problem is transformed into a simpler one with auxiliary variables V, W and Z. The augmented Lagrangian that uses additional quadratic penalty terms with penalty parameter ρ is further computed as follows:

$$L(\Phi,\Theta,V,W,Z)=\mathcal{L}_D(\Phi,\Theta)+\mathrm{tr}(y^{(1)}(Z-f(X))^T)+\frac{\rho}{2}||Z-f(X)||_2^2$$
$$+\frac{\beta}{2}\sum_s^{\mathcal{S}}\sum_{i,j}^{C_k^2}\|Z_s(V_{s,i}-V_{s,j})^T-\frac{1}{N_s}\sum_c^{\mathcal{S}}adj(s,c)Z_c(W_{c,i}-W_{c,j})^T\|_2^2+$$
$$\mathrm{tr}(y^{(2)}(\Theta-V)^T)+\frac{\rho}{2}||\Theta-V||_2^2+\mathrm{tr}(y^{(3)}(\Theta-W)^T)+\frac{\rho}{2}||\Theta-W||_2^2$$

where the $tr(\cdot)$ operator denotes the trace of the matrix.

Algorithm 1: The Proposed Algorithm

```
Require: $X, Y, \rho, \beta, \lambda$
Ensure: solution $\Phi, \Theta$
 1: initialize $\Phi^0, \Theta^0, V^0, W^0, Z^0, y^{(1)0}, y^{(2)0}, y^{(3)0}, i=0$
 2: repeat
 3:   % Solve subproblem of variable $\Phi, \Theta$ by fixing the other variables
 4:   $\Phi^i, \Theta^i \Leftarrow$
      $\mathrm{argmin}_{\Phi,\Theta}\, \mathcal{L}_D(\Phi,\Theta) + \mathrm{tr}(y^{(1)}(Z-f(X))^T)+\frac{\rho}{2}||Z-f(X)||_2^2 +$
      $\mathrm{tr}(y^{(2)}(\Theta-V)^T)+\frac{\rho}{2}||\Theta-V||_2^2+\mathrm{tr}(y^{(3)}(\Theta-W)^T)+\frac{\rho}{2}||\Theta-W||_2^2$
 5:   for $s \Leftarrow 1$ to $K$ do
 6:     % Get the analytical solution of $V_s$ by setting $\nabla_{V_s} L(\Phi,\Theta,V,W,Z)=0$
 7:     $V_s^i \Leftarrow \left(\beta(Z_s^T Z_s) \otimes (MM^T) + \rho I\right)^{-1}$
        $vec\left(y_s^{(2)} + \rho\Theta_s + \beta M \left(\frac{1}{N_s}\sum_c^{\mathcal{S}} adj(s,c)Z_c W_c^T M\right)^T Z_s\right)$
 8:   end for
 9:   for $c \Leftarrow 1$ to $K$ do
10:     % Get the analytical solution of $W_c$ by setting $\nabla_{W_c} L(\Phi,\Theta,V,W,Z)=0$
11:     $W_c^i \Leftarrow \left(\beta\sum_s^{\mathcal{S}} \frac{adj(s,c)^2}{N_s^2}(Z_c^T Z_c) \otimes (MM^T)+\rho I\right)^{-1}$
        $vec\left(y_c^{(3)}+\rho\Theta_c-\beta\sum_s^{\mathcal{S}} M\left(\frac{1}{N_s}\sum_{i\neq c}^{\mathcal{S}} adj(s,i)Z_i W_i^T M-Z_s V_s^T M\right)^T Z_c\right)$
12:   end for
13:   for $s \Leftarrow 1$ to $K$ do
14:     % Get the analytical solution of $Z_s$ by setting $\nabla_{Z_s} L(\Phi,\Theta,V,W,Z)=0$
15:     $Z_s^i \Leftarrow \left(-y_s^{(1)}+\rho f(X_s)+\beta\left(\frac{1}{N_s}\sum_c^{\mathcal{S}} adj(s,c)Z_c W_c^T M\right) M^T V_s\right)$
        $\left(\beta V_s^T M M^T V_s + \rho I\right)^{-1}$
16:   end for
17:   $y^{(1)i} \Leftarrow y^{(1)} + \rho(Z - f(X))$        % Update dual variable $y^{(1)}$
18:   $y^{(2)i} \Leftarrow y^{(2)} + \rho(\Theta - V)$           % Update dual variable $y^{(2)}$
19:   $y^{(3)i} \Leftarrow y^{(3)} + \rho(\Theta - W)$           % Update dual variable $y^{(3)}$
20:   $i \Leftarrow i + 1$
21: until convergence
```

The pseudo-code of the proposed algorithm is summarized in **Algorithm 1**. The parameter set $\{\Phi, \Theta, V, W, Z, y^{(1)}, y^{(2)}, y^{(3)}\}$ is alternately solved by the proposed algorithm until convergence is achieved. Lines 3-15 show the alternating optimization for each of the variables. $M \in \mathbb{R}^{k\times C_k^2}$ is an auxiliary matrix to help make the computation in matrix format, as elaborated in the supplementary material.

Experiments

Dataset and Experiment Setup

In this study, five datasets from civil unrest forecasting and one dataset from air pollution event forecasting are used for the experimental evaluations. All the experiments were conducted on a 64-bit machine with Intel(R) core(TM) quad-core processor (i7CPU 2.5GHz) and 16GB memory.

Civil Unrest Datasets: These datasets were obtained from 5 different countries in Latin America, namely Brazil, Colombia, Mexico, Paraguay, and Venezuela. Data sources from Twitter are adopted as the model inputs. In each case the data for the period from July 1, 2013 to February 9, 2014 is used for training and validation, where the validation set consists of a randomly chosen 30% of the data, and the rest is used for training; the data from February 10, 2014 to December 31, 2014 is used for the performance evaluation. The event forecasting results are validated against a well-established labeled events set, the Gold Standard Report (GSR) (GSR Dataset). GSR is a collection of civil unrest news reports from the most influential newspaper outlets in Latin America (O'Connor et al. 2010). The event subtype for the civil unrest dataset is the event primary population type (i.e. 'Business', 'Education' etc.). An example of a labeled GSR event is given by the tuple: (City="Maracaibo", State ="Zulia", Country = "Venezuela", Date = "2013-01-19", Event subtype="Education").

Air Pollution Dataset: The dataset used for air pollution event forecasting covers the major cities in China. Air quality information about the concentration of pollutant sources (such as $PM2.5$ and $PM10$) is used as the data source. The dataset contains about one-year air condition records for major cities in China from July 2016 to July 2017. The first half of the data (for the year 2016) is used for training and validation, where the validation set consists of a randomly chosen 30% of the data, and the rest is used for training; the data for 2017 is used for performance evaluation. To further enrich the experiment and assess the prediction power of our proposed model, 4 different settings for the prediction lead time p (1 day, 3 days, 5 days, and 7 days) are utilized in the experiment. The forecasting results for the most important primary pollutants are validated against the corresponding air quality statistics reported by the corresponding cities' local air quality monitoring stations, together with each city's Environmental Monitoring Center. The Environmental Monitoring Centers publish daily summaries of the primary pollutants affecting their cities. The event subtype is the most important primary pollutant (such as $PM2.5$, $PM10$, O_3 and $None$, with the latter indicating good air quality with no major pollutants present). An example of an air pollution daily report is: (City = "Beijing", Station = "Temple of Heaven", Date = "01-01-2017", Primary Pollutant = "$PM2.5$").

Parameter Setting: The hyper-parameters and network structure are chosen via a grid search based on model performance on the validation set. For all neural network based models, fully connected layers with sigmoid activation function are used. More detailed parameter settings and sensitivity analysis are presented in the supplemental material.

Performance Evaluation: To evaluate the model performance, macro-average precision, recall and F1-Score are used here to provide an overall measure of model performance across all event subtype classes. In addition, we also introduce the Receiver Operating Characteristic (ROC) curve to further evaluate the overall prediction power.

Baselines for comparison: The performance of the proposed model is compared with baselines as well as existing state of the art methods, namely: *SVC1V1* (Support Vec-

Table 1: Performance comparison for the civil unrest datasets (macro Precision, Recall and F1).

Method	Brazil	Colombia	Mexico	Paraguay	Venezuela
SVC1VA	0.2318,0.2479,0.2368	0.2374,0.2673,0.2447	0.1798,0.1991,0.1738	0.2009,0.2396,0.2055	0.2136,0.2348,0.2069
SVC1V1	0.2444,0.2582,0.2465	0.2062,0.2096,0.1995	0.1651,0.1600,0.1511	0.2058,0.2715,0.2152	0.2118,0.2481,0.2058
SR	0.2131,0.2525,0.2247	0.2496,0.2840,0.2545	0.1781,0.1888,0.1676	0.2212,0.2644,0.2287	0.2239,0.2507,0.2191
SIMDA-SR	0.2586,0.2699,0.2560	0.2568,0.2799,0.2645	0.2106,0.1897,0.1849	0.2378,0.2935,0.2402	0.2538,**0.2661**,0.2326
MLP-1	0.2423,0.2358,0.2359	0.2369,0.2354,0.2357	0.1800,0.1957,0.1715	0.2160,0.3145,0.2234	0.2174,0.2200,0.2155
MLP-2	0.2512,0.2575,0.2530	0.2594,0.2736,0.2634	0.1757,0.1534,0.1608	0.2300,0.2694,0.2307	0.2180,0.2311,0.2152
MLP-3	0.2699,0.2590,0.2643	0.2400,0.2628,0.2436	0.1842,0.1539,0.1675	0.2133,0.2049,0.2084	0.2174,0.2200,0.2155
SBM-1	0.2821,0.2634,0.2696	**0.2956**,0.2701,0.2762	**0.2237**,0.2051,0.2121	0.2447,0.3655,0.2543	0.2212,0.2115,0.2122
SBM-2	0.2560,0.2737,0.2597	0.2919,0.2637,0.2732	0.2104,0.1951,0.2009	0.2363,0.2971,0.2416	0.2455,0.2505,0.2286
SBM-3	0.2821,0.2637,0.2714	0.2759,**0.3176**,**0.2863**	0.2060,0.1793,0.1908	0.2392,0.2459,0.2369	0.2545,0.1910,0.2162
SIMDA-1	**0.2848**,**0.2804**,**0.2788**	**0.3067**,0.2761,**0.2845**	0.2187,0.2070,**0.2123**	0.2467,**0.3749**,**0.2562**	**0.2684**,0.2422,**0.2477**
SIMDA-2	**0.3558**,**0.2887**,**0.2779**	0.2648,0.3130,0.2670	**0.2252**,**0.2110**,**0.2176**	**0.2543**,0.3373,**0.2638**	**0.2704**,0.2421,**0.2471**
SIMDA-3	0.2828,0.2641,0.2712	0.2689,**0.3152**,0.2710	0.2081,**0.2338**,0.2000	**0.2473**,**0.4482**,0.2532	0.2178,**0.2571**,0.2174

Table 2: China air pollution event forecasting dataset with various prediction lead times (macro Precision, Recall and F1).

Method	1-day	3-days	5-days	7-days
SVC1VA	0.4966,0.5255,0.5009	0.4362,0.4768,0.4309	0.3940,0.3946,0.3872	0.4334,0.4553,0.4240
SVC1V1	0.5700,0.5716,0.5652	0.4532,0.4849,0.4565	0.4361,0.4545,0.4380	0.4351,0.4412,0.4302
SR	0.4254,0.4338,0.4287	0.4082,0.4229,0.4102	0.3949,0.4208,0.3974	0.4126,0.4277,0.4104
SIMDA-SR	0.5290,**0.6436**,0.5572	0.4256,**0.6395**,0.4293	0.4281,**0.6350**,0.4236	0.4541,**0.6863**,0.4412
MLP-1	0.5640,0.5625,0.5594	0.4679,0.4809,0.4614	0.4596,0.4761,0.4451	0.4646,0.4684,0.4592
MLP-2	**0.6108**,0.5567,0.5693	0.4687,0.4805,0.4638	0.4378,0.4359,0.4308	0.4605,0.4472,0.4504
MLP-3	0.5739,0.5873,0.5719	0.4989,0.4916,0.4902	0.4848,0.4683,0.4718	0.4597,0.4537,0.4364
SBM-1	0.5710,0.6162,0.5812	**0.5718**,0.5230,0.5162	**0.5692**,0.5075,0.5134	**0.5763**,0.5343,0.4896
SBM-2	0.5383,0.5981,0.5509	0.4630,**0.6396**,0.4880	0.4802,0.6211,0.4997	0.5070,0.6457,0.5256
SBM-3	0.5284,0.6085,0.5526	0.5154,0.5426,0.5035	0.5089,0.6331,**0.5236**	0.5271,0.5631,0.5184
SIMDA-1	0.5558,0.5668,0.5560	0.4761,0.5704,0.5046	0.4878,**0.6562**,0.5085	0.4738,**0.6539**,0.4698
SIMDA-2	0.5605,**0.6556**,**0.5863**	0.4932,0.6186,**0.5290**	0.4935,0.5289,0.4991	**0.5627**,0.6390,**0.5868**
SIMDA-3	**0.5979**,0.6364,**0.6002**	**0.5633**,0.5776,**0.5431**	**0.5256**,0.5851,**0.5300**	0.5138,0.6310,**0.5425**

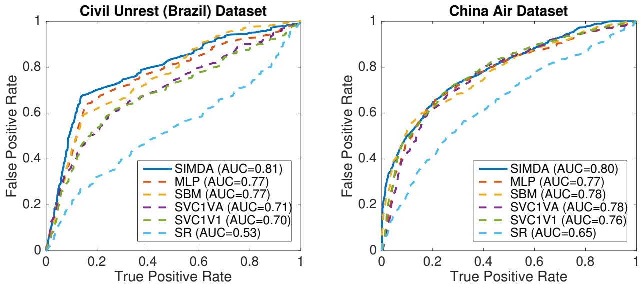

Figure 3: Macro-average ROC comparison

tor Classifier with OneVsOne) and *SVC1VA* (Support Vector Classifier with OneVsAll) (Hsu and Lin 2002), *SR* (Softmax Regression) (Nasrabadi 2007; Chen et al. 2013), *MLP* (MultiLayer Perceptron)(Rumelhart, Hinton, and Williams 1985) and *SBM* (Shared-Bottom Model) (Caruana 1998; Caruna 1993). The detailed introduction and hyper-parameter settings are included in the supplemental material.

Performance

Tables 1 and 2 show the performance for all the methods on all the datasets over all the event subtypes based on macro-average precision, recall and F1-score. For neural network based models the numbers attached along with the model name are the number of hidden layers, notice that SIMDA-SR is SIMDA framework used with Softmax Regression (i.e. without hidden-layers) . In both tables, the best results for each dataset are highlighted in bold face and underlined; the second best are in bold face only.

Table 1 shows that SIMDA framework used along with deep architectures performs consistently well across all the different countries, being the best in Brazil, Mexico, Paraguay, and Venezuela and competitive in Colombia. It outperforms the baseline models by 10% - 25% among macro-average precision, recall and F1-score. The baseline SBM also achieves good scores, but is overall not as competitive as SIMDA. This is largely because SIMDA utilizes geo-information by including the proposed spatial correlation based constraint. Interestingly, SIMDA largely outperforms the baselines on the Venezuela dataset, but achieves only competitive results on the Colombia dataset compared with SBM. Examining the dataset, 11 of the 14 cities have incomplete event subtype classes in the Venezuela dataset, nearly 80% of the total, while only 8 out of 13 cities have incomplete event subtype classes in the Colombia dataset, around 60%. This may suggest that the spatial regularization term in SIMDA improves the performance substantially when there is more serious incompleteness of classes.

Table 2 also demonstrate the effectiveness of the proposed methods in the domain of air pollution event forecasting with different prediction lead times. SIMDA used along with deep architectures outperforms the baseline models consistently by 5%-10% in terms of the F1-score and achieves the top performance for both precision and recall. The results presented in this table also highlight the increasing difficulty of predictions with longer lead times, as forecasting long-term future events introduces considerably more uncertainty. However, the proposed model behaves stably and suffers from less decline in terms of its overall performance compared with the other methods. For instance, the F1-score only decreases by about 10% for the SIMDA-3 model, while other baselines decrease by about 15%-30%. This may suggest that the proposed spatial regularization term in SIMDA improves the robustness of the deep model substantially, enabling it to capture more long-term dependencies of the data and the corresponding event subtypes.

The experimental results in both Table 1 and 2 show that overall shallow models such as SR, SVM based models and SIMDA-SR perform worse than deep models with hidden layers such as MLP, SBM and SIMDA-3. This is largely because shallow models cannot discriminate the subtle differ-

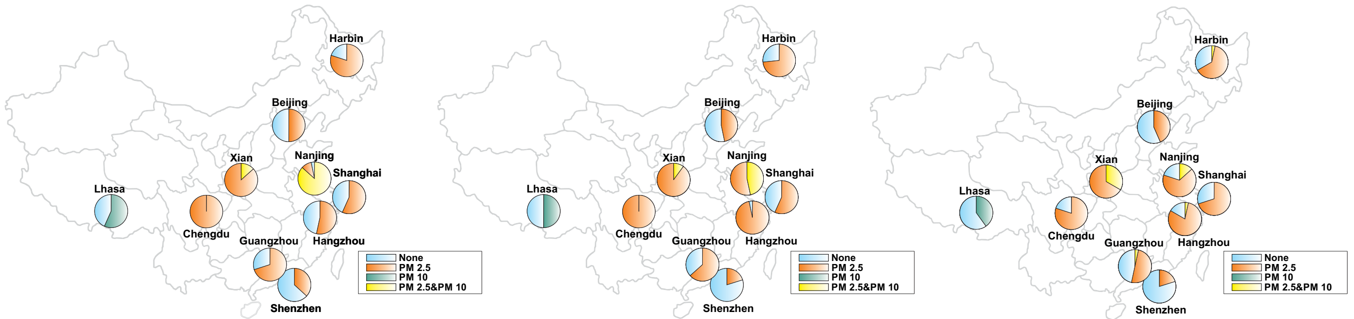

(a) Primary Pollutant Distribution Predicted by SBM

(b) Primary Pollutant Distribution Predicted by SIMDA

(c)The Ground Truth Primary Pollutant Distribution

Figure 4: Comparison of pollutant subtype distribution predicted by SBM and SIMDA of major cities in China

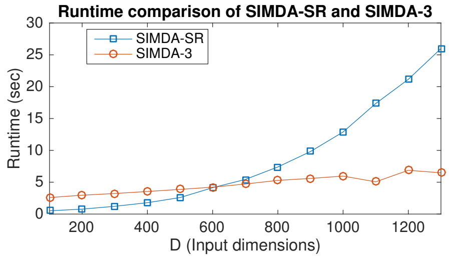

Figure 5: Runtime comparison of SIMDA-SR and SIMDA-3

ences between event subtype patterns very well. Notice that among the shallow models, SIMDA-SR still outperforms all other baselines most of the time, which further demonstrates the effectiveness of the proposed spatial regularization even on shallow models on various application domains.

To further evaluate the overall prediction power of the SIMDA model, the Receiver Operating Characteristic (ROC) curve is also introduced for comparison, as shown in Figure 3. Here, the Brazil dataset is used to represent the Civil Unrest dataset, other datasets follow the similar trends. The China Air dataset has a lead time of 7 days. The proposed SIMDA model curve is the blue solid line and those for the baseline models are shown as dashed lines. The Area Under Curve (AUC) for each curve is provided in the legend. Notice that for neural network based models, only those giving the best AUC scores are shown here. The curves for the Civil Unrest dataset on the left clearly show that the SIMDA model achieves the best ROC curve, with an AUC score of 0.81. This is also the case for the China air pollution dataset, where the SIMDA model again achieves the highest AUC score of 0.80. This further demonstrates the effectiveness and overall prediction power of the proposed SIMDA model.

Scalability

Figure 5 compares the run time of SIMDA-SR with softmax regression and SIMDA-3 with three hidden layers in its neural network architecture on one step of the ADMM iteration. The run time for SIMDA-SR increases quadratically with the number of input dimensions, starting from only 0.5 second with 100 dimensions and rising to around 26 seconds with 1300 dimensions. On the other hand, the run time for the 3 hidden layer SIMDA increases linearly starting from 2.6 seconds for 100 dimensions and then climbing to 6 seconds with 1300 input dimensions, when the number of neurons of the the hidden layers remain unchanged. This demonstrates that the generalized SIMDA framework enjoys better scalability in terms of time complexity when dealing with high dimensional complex real world data.

The Effect of Subtype Pattern Regularization

This section validates the effectiveness of the deep regularization term regarding the event subtype patterns in the SIMDA model. Looking at the China air pollution event forecasting dataset, Figure 4 compares the pollutant subtype patterns in terms of the class distribution predicted by the baseline SBM (i.e., without regularization) and SIMDA (i.e. with regularization), with Figure 4 (a) and (b), respectively, showing the models' predicted event subtype distributions for each task (city) in China. Figure 4(c) shows the ground truth distribution for the same period. Overall, Figure 4(b) shows a better fit for the subtype distribution among the different cities than Figure 4(a). This indicates that with the help of the spatial regularization term, SIMDA was able to learn a better class distribution even when the event subtypes are imbalanced and incomplete. For instance, for the city Nanjing, with no spatial regularization, SBM over-fits the training data severely and forecasts the future subtype as predominantly "PM2.5&PM10" which diverges significantly from the ground truth distribution. In contrast, SIMDA not only learns from task specific training data, but also regularizes the model by sharing adjacent tasks' event subtype probability ratios. Consequently, the SIMDA model over-fits less on subtype "PM2.5&PM10" and successfully forests "PM2.5" as the majority subtype during the test period, which is a closer fit to the ground truth distribution shown in Figure 4(c).

Conclusions

Beyond merely predicting the occurrence of future events, effective forecasting of event subtypes provides valuable information to practitioners and enables them to allocate appropriate amounts and types of resources to manage and ameliorate social risks. To achieve this objective, this paper proposes a novel Spatial Incomplete Multi-task Deep leArning (SIMDA) framework that characterizes spatial heterogeneity, task label incompleteness, and event subtype pattern correlations. An efficient algorithm is proposed to handle this non-convex and strongly coupled model objective. Extensive experiments on six real-world datasets demonstrate that the proposed model outperforms other baseline methods in multiple application domains.

References

Achrekar, H.; Gandhe, A.; Lazarus, R.; Yu, S.-H.; and Liu, B. 2011. Predicting flu trends using twitter data. In *INFOCOM WKSHPS*, 702–707. IEEE.

Ando, R. K., and Zhang, T. 2005. A framework for learning predictive structures from multiple tasks and unlabeled data. *Journal of Machine Learning Research* 6(Nov):1817–1853.

Bellman, R. 2013. *Dynamic programming*. Courier Corporation.

Boyd, S.; Parikh, N.; Chu, E.; Peleato, B.; and Eckstein, J. 2011. Distributed optimization and statistical learning via the alternating direction method of multipliers. *Foundations and Trends® in Machine Learning* 3(1):1–122.

Caruana, R. 1998. Multitask learning. In *Learning to learn*. Springer. 95–133.

Caruna, R. 1993. Multitask learning: A knowledge-based source of inductive bias. In *Machine Learning: Proceedings of the Tenth International Conference*, 41–48.

Chen, Z.; Xie, Y.; Cheng, Y.; Zhang, K.; Agrawal, A.; Liao, W.-k.; Samatova, N. F.; and Choudhary, A. N. 2013. Forecast oriented classification of spatio-temporal extreme events. In *IJCAI*, 2952–2954.

Cressie, N. 2015. *Statistics for spatial data*. John Wiley & Sons.

Duong, L.; Cohn, T.; Bird, S.; and Cook, P. 2015. Low resource dependency parsing: Cross-lingual parameter sharing in a neural network parser. In *ACL 2015 (Volume 2: Short Papers)*, volume 2, 845–850.

Evgeniou, T., and Pontil, M. 2004. Regularized multi–task learning. In *KDD 2004*, 109–117. ACM.

Gao, Y., and Zhao, L. 2018. Incomplete label multi-task ordinal regression for spatial event scale forecasting. In *The Thirty-Third AAAI Conference on Artificial Intelligence*.

GSR Dataset. https://dataverse.harvard.edu/dataset.xhtml?persistentId=doi:10.7910/DVN/EN8FUW. accessed Sep 2018.

Haasdonk, B., and Bahlmann, C. 2004. Learning with distance substitution kernels. In *Joint Pattern Recognition Symposium*, 220–227. Springer.

Hornik, K. 1991. Approximation capabilities of multilayer feedforward networks. *Neural networks* 4(2):251–257.

Hsu, C.-W., and Lin, C.-J. 2002. A comparison of methods for multiclass support vector machines. *IEEE transactions on Neural Networks* 13(2):415–425.

Khezerlou, A. V.; Zhou, X.; Li, L.; Shafiq, Z.; Liu, A. X.; and Zhang, F. 2017. A traffic flow approach to early detection of gathering events: Comprehensive results. *ACM Transactions on Intelligent Systems and Technology (TIST)* 8(6):74.

Kiaee, F.; Gagné, C.; and Abbasi, M. 2016. Alternating direction method of multipliers for sparse convolutional neural networks. *arXiv preprint arXiv:1611.01590*.

Misra, I.; Shrivastava, A.; Gupta, A.; and Hebert, M. 2016. Cross-stitch networks for multi-task learning. In *CVPR 2016*, 3994–4003.

Nasrabadi, N. M. 2007. Pattern recognition and machine learning. *Journal of electronic imaging* 16(4):049901.

Ning, Y.; Muthiah, S.; Rangwala, H.; and Ramakrishnan, N. 2016. Modeling precursors for event forecasting via nested multi-instance learning. In *KDD 2016*, 1095–1104. ACM.

O'Connor, B.; Balasubramanyan, R.; Routledge, B. R.; and Smith, N. A. 2010. From tweets to polls: Linking text sentiment to public opinion time series. *ICWSM* 11(122-129):1–2.

Ramakrishnan, N.; Butler, P.; Muthiah, S.; Self, N.; Khandpur, R.; Saraf, P.; Wang, W.; Cadena, J.; Vullikanti, A.; Korkmaz, G.; et al. 2014. 'beating the news' with embers: forecasting civil unrest using open source indicators. In *KDD 2014*, 1799–1808. ACM.

Rumelhart, D. E.; Hinton, G. E.; and Williams, R. J. 1985. Learning internal representations by error propagation. Technical report, California Univ San Diego La Jolla Inst for Cognitive Science.

Sun, J.; Li, H.; Xu, Z.; et al. 2016. Deep admm-net for compressive sensing mri. In *Advances in Neural Information Processing Systems*, 10–18.

Thrun, S., and OSullivan, J. 1998. Clustering learning tasks and the selective cross-task transfer of knowledge. In *Learning to learn*. Springer. 235–257.

Vahedian, A.; Zhou, X.; Tong, L.; Li, Y.; and Luo, J. 2017. Forecasting gathering events through continuous destination prediction on big trajectory data. In *Proceedings of the 25th ACM SIGSPATIAL International Conference on Advances in Geographic Information Systems*, 34. ACM.

Wu, L.; Yen, I. E.-H.; Xu, F.; Ravikuma, P.; and Witbrock, M. 2018. D2ke: From distance to kernel and embedding. *arXiv preprint arXiv:1802.04956*.

Xia, X.; Qi, Q.; Liang, H.; Zhang, A.; Jiang, L.; Ye, Y.; Liu, C.; and Huang, Y. 2016. Pattern of spatial distribution and temporal variation of atmospheric pollutants during 2013 in shenzhen, china. *ISPRS International Journal of Geo-Information* 6(1):2.

Xu, K.; Wu, L.; Wang, Z.; and Sheinin, V. 2018. Graph2seq: Graph to sequence learning with attention-based neural networks. *arXiv preprint arXiv:1804.00823*.

Yang, Y., and Hospedales, T. 2016. Deep multi-task representation learning: A tensor factorisation approach. *arXiv preprint arXiv:1605.06391*.

Yuan, Z.; Zhou, X.; and Yang, T. 2018. Hetero-convlstm: A deep learning approach to traffic accident prediction on heterogeneous spatio-temporal data. In *KDD 2018*, 984–992. ACM.

Zhao, L.; Chen, F.; Lu, C.-T.; and Ramakrishnan, N. 2015a. Spatiotemporal event forecasting in social media. In *SDM 2015*, 963–971. SIAM.

Zhao, L.; Sun, Q.; Ye, J.; Chen, F.; Lu, C.-T.; and Ramakrishnan, N. 2015b. Multi-task learning for spatio-temporal event forecasting. In *KDD 2015*, 1503–1512. ACM.

Zheng, Y.; Liu, F.; and Hsieh, H.-P. 2013. U-air: When urban air quality inference meets big data. In *KDD 2013*, 1436–1444. ACM.